Wavelength-selective directional coupling with dielectric-loaded plasmonic waveguides

Zhuo Chen,[1] Tobias Holmgaard,[1] Sergey I. Bozhevolnyi,[1,2,*] Alexey V. Krasavin,[3] Anatoly V. Zayats,[3] Laurent Markey,[4] and Alain Dereux[4]

[1]*Department of Physics and Nanotechnology, Aalborg University, Skjernvej 4A, DK-9220 Aalborg Øst, Denmark*
[2]*Institute of Sensors, Signals and Electrotechnics (SENSE), University of Southern Denmark, Niels Bohrs Allé 1, DK-5230 Odense M, Denmark*
[3]*Centre for Nanostructured Media, International Research Centre for Experimental Physics, The Queen's University of Belfast, Belfast BT7 1NN, United Kingdom*
[4]*Institut Carnot de Bourgogne, UMR 5209 CNRS—Université de Bourgogne, 9 Avenue A. Savary, BP 47 870, F-21078 Dijon CEDEX, France*
**Corresponding author: seib@sense.sdu.dk*

Received November 10, 2008; revised December 18, 2008; accepted December 18, 2008; posted December 22, 2008 (Doc. ID 103903); published January 26, 2009

We consider wavelength-selective splitting of radiation using directional couplers (DCs) formed by dielectric-loaded surface-plasmon-polariton waveguides (DLSPPWs). The DCs were fabricated by depositing subwavelength-sized polymer ridges on a gold film using large-scale UV photolithography and characterized at telecommunications wavelengths with near-field microscopy. We demonstrate a DLSPPW-based 45-μm-long DC comprising 3 μm offset S bends and 25-μm-long parallel waveguides that changes from the "through" state at 1500 nm to 3 dB splitting at 1600 nm, and show that a 50.5-μm-long DC should enable complete separation of the radiation channels at 1400 and 1620 nm. The DC performance is found to be in good agreement with full vectorial three-dimensional finite-element simulations.

OCIS codes: 240.6680, 130.3120, 130.5460.

Surface-plasmon polaritons (SPPs), light waves coupled to free-electron oscillations in metal [1], can be laterally confined below the diffraction limit using subwavelength metal structures [2]. Plasmonic components open an appealing perspective of combining the high operational bandwidth of photonic components with the subwavelength dimensions of SPP waveguides [1,2]. Recently developed dielectric-loaded SPP waveguides (DLSPPWs), utilizing high effective indexes of SPP modes guided by dielectric ridges on smooth metal films [3–7], represent an attractive alternative to other plasmonic technologies by virtue of being naturally compatible with different dielectrics and large-scale industrial fabrication using UV lithography [8–10]. Preliminary investigations indicated that DLSPPW-based components feature relatively low bend and propagation losses [9,10], but their potential for wavelength selection, a crucial functionality for any photonic circuit, has so far not been explored.

Wavelength-selective plasmonic components generally feature more complicated geometry [2], thereby imposing additional requirements to the accuracy of fabrication. In our case, one should also bear in mind a (diffraction) limited resolution of UV lithography [9] employed for the DLSPPW fabrication. Taking into account a rather good performance of recently investigated DLSPPW-based S bends [9], we suggest making use of wavelength-dependent behavior of directional couplers (DCs) [11] for the selection and spatial separation of radiation channels at different wavelengths. Note that the wavelength dispersion of directional coupling using DLSPPWs has not been considered in previous publications [6,7]. Here we report on the fabrication, characterization, and modeling of DLSPPW-based wavelength-selective DCs operating at telecommunication wavelengths.

All waveguide structures were fabricated using deep UV lithography (wavelength of ~250 nm) with a Süss Microtech MJB4 mask aligner in the vacuum contact mode and a ~550 nm thick layer of polymethyl-methacrylate (PMMA) resist spin coated on a 60 nm thin gold film, which was supported by a thin glass substrate. Typically, the width of the produced waveguides, inspected with scanning electron microscopy (SEM), was close to 500 nm ensuring the single-mode (and close to optimum) DLSPPW operation [5]. The performance of the fabricated components was characterized using a scanning near-field optical microscope (SNOM), operating in collection mode with an uncoated fiber tip used as a probe, and an arrangement for SPP excitation (at $\lambda = 1500-1620$ nm) in the Kretschmann–Raether configuration, as described in detail elsewhere [10]. All waveguide structures were connected to funnel structures [Fig. 1(a)], facilitating efficient excitation of the DLSPPW mode [8], with the further improvement in that the DLSPPW mode was excited directly inside the taper by matching the excitation angle (under total internal reflection), resulting in SNOM images of high quality [9,10]. We found that all structures exhibited the DLSPPW propagation length of ~50 μm, slightly increasing with the wavelength [10].

Several DLSPPW-based 45-μm-long DCs, comprising 3 μm offset, 10-μm-long (input and output) S bends, having different center-to-center separations, $S = 800$, 900, and 1000 nm, between 25-μm-long parallel waveguides were fabricated and characterized with the SNOM at different wavelengths (Fig. 1). It

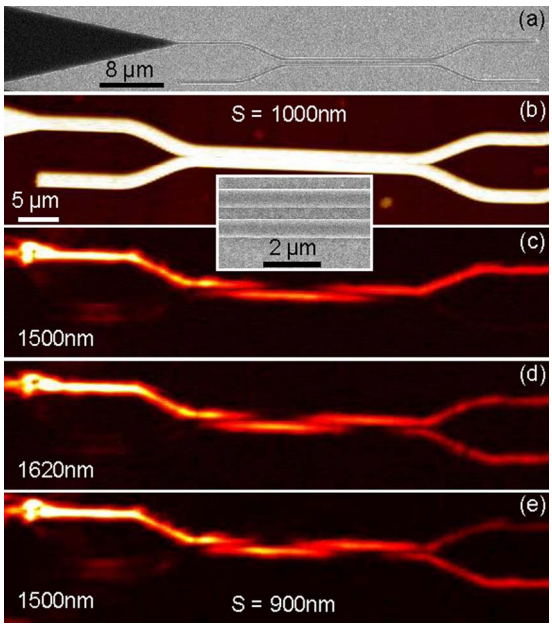

Fig. 1. (Color online) (a) Scanning electron microscope image of the fabricated DC showing the funnel structure facilitating the DLSPPW excitation. (b) Topographical and (c)–(e) near-field optical [λ=(c) 1500, (d) 1620, and (e) 1500 nm] SNOM images of 45 μm long DCs with the separations (b)–(d) $S=1000$ nm along with an inset showing SEM image of the coupling region and (e) $S=900$ nm.

was observed that the coupling length l_c (i.e., the interaction length needed to completely transfer the power from one waveguide to another) depends strongly on the separation [Figs. 1(c) and 1(e)] and varies noticeably with the wavelength, influencing the power level in the output waveguides [Figs. 1(c) and 1(d)]. At the same time, the total DC transmission evaluated using the input and output waveguide cross sections (separated by $L=45$ μm) is practically wavelength independent maintaining the level of ~0.23, a value that is consistent with the loss incurred by 25-μm-long propagation (~40%) and two S bends (~35% per bend) [9]. One can thereby conclude that the performance of the fabricated DCs is not degraded owing to fabrication errors, an important circumstance that is achieved because the DC design does not contain critical elements requiring high-resolution lithography.

To get further insight into the DLSPPW-based DC operation, we conducted full three-dimensional finite-element method (3D-FEM) simulations of the DC operation [6] that allowed us to retrieve the coupling length dispersion. It is seen that the simulation results agree well with the experimental values obtained directly from the SNOM images (Fig. 2). This dispersion was used to calculate the normalized output signals, i.e., straight T_s and cross T_c transmissions, with only one waveguide being excited at the input,

$$T_{s,c}(\lambda) = (T_{\text{bend}})^2 \exp\left(-\frac{L_p}{L_{SP}}\right)\left\{\begin{matrix}\cos^2\\ \sin^2\end{matrix}\left(\frac{\pi L_i}{2l_c(\lambda)}\right)\right\}, \quad (1)$$

where the first factor reflects the S-bend transmission, the second one reflects the power loss incurred

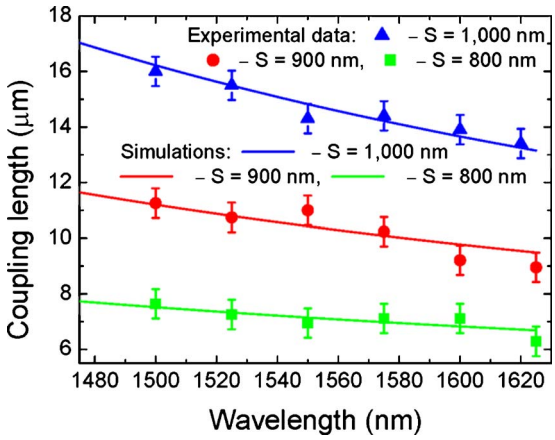

Fig. 2. (Color online) DC coupling length evaluated for different wavelengths and separations directly from SNOM images similar to those shown in Figs. 1(c)–1(e) and calculated with 3D-FEM simulations.

by the propagation through the section of parallel waveguides (of length L_p), and L_i denotes the effective interaction length; typically, $L_i > L_p$ due to the additional mode coupling in the S bends [11]. Using the already known parameters, $T_{\text{bend}} \sim 0.65$ (evaluated using the available experimental data [9]), $L_p = 25$ μm and $l_c(\lambda)$ for $S=1000$ nm (Fig. 2), we found that the interaction length $L_i \cong 34$ μm results in good agreement (Fig. 3) between the calculated [Eq. (1)] output signals and the values obtained from SNOM images, similar to those shown in Fig. 1. Using the obtained results one can *design* a DC structure that would ensure spatial separation of radiation corresponding to different bands used in optical telecommunications. For example, an increase of the length of parallel section by ≅5.5 μm for the DC with $S=1000$ nm would enable spatial separation of the wavelengths of 1400 and 1620 nm (belonging to E and L bands) as seen from the calculations using Eq. (1) with $L_p=30.5$ μm and $L_i \cong 39.5$ μm (Fig. 3).

In conclusion, we have considered the usage of DC wavelength dispersion for the selection and spatial

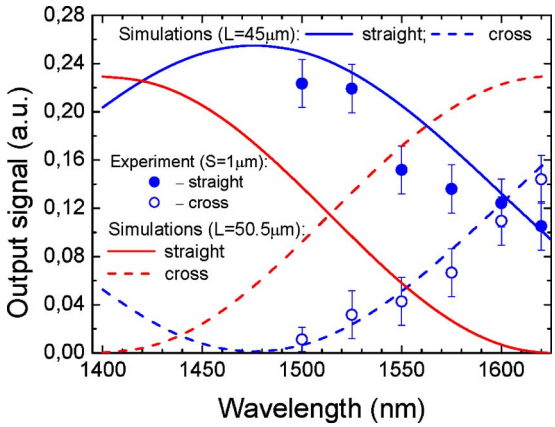

Fig. 3. (Color online) DC output signals normalized with respect to the input when exciting only one waveguide, determined experimentally from SNOM images similar to those shown in Figs. 1(c)–1(e) and calculated using Eq. (1) and the DC coupling length dispersion shown in Fig. 2.

separation of radiation channels at different wavelengths. Using industrially compatible large-scale UV-lithography-based fabrication and exploiting the principles of DLSPPW-based plasmonic technology, we have fabricated and characterized wavelength-selective DCs operating at telecommunications wavelengths. We have demonstrated a DLSPPW-based 45-μm-long DC comprising 3 μm offset S bends and 25-μm-long parallel waveguides that changes from the through state at 1500 nm to 3 dB splitting at 1600 nm and have shown that a 50.5-μm-long DC should enable complete separation of the radiation channels at 1400 and 1620 nm (belonging to E and L bands). The performance of the considered structures could be further improved by fine tuning the DC parameters so as to achieve overall optimization (e.g., with the 3D-FEM simulations) with respect to the wavelength selection and insertion loss. Taking into account the fact that this technology is naturally compatible with different dielectrics, one can envisage the development of ultracompact plasmonic components utilizing thermo-optical, electro-optical, magneto-optical, acousto-optical, and nonlinear optical effects as well as being integrated with electrical circuits.

This work was supported by EC FP6 STREP PLASMOCOM. A. V. Krasavin and A. V. Zayats also acknowledge the financial support from the Engineering and Physical Sciences Research Council (EPSRC) (UK).

References

1. W. L. Barnes, A. Dereux, and T. W. Ebbesen, Nature **424**, 824 (2003).
2. T. W. Ebbesen, C. Genet, and S. I. Bozhevolnyi, Phys. Today **61**, 44 (May 2008).
3. C. Reinhardt, S. Passinger, B. N. Chichkov, C. Marquart, I. P. Radko, and S. I. Bozhevolnyi, Opt. Lett. **31**, 1307 (2006).
4. B. Steinberger, A. Hohenau, H. Ditlbacher, A. L. Stepanov, A. Drezet, F. R. Aussenegg, A. Leitner, and J. R. Krenn, Appl. Phys. Lett. **88**, 094104 (2006).
5. T. Holmgaard and S. I. Bozhevolnyi, Phys. Rev. B **75**, 245405 (2007).
6. A. V. Krasavin and A. V. Zayats, Appl. Phys. Lett. **90**, 211101 (2007).
7. B. Steinberger, A. Hohenau, H. Ditlbacher, F. R. Aussenegg, A. Leitner, and J. R. Krenn, Appl. Phys. Lett. **91**, 081111 (2007).
8. T. Holmgaard, S. I. Bozhevolnyi, L. Markey, and A. Dereux, Appl. Phys. Lett. **92**, 011124 (2008).
9. T. Holmgaard, Z. Chen, S. I. Bozhevolnyi, L. Markey, A. Dereux, A. V. Krasavin, and A. V. Zayats, Opt. Express **16**, 13585 (2008).
10. T. Holmgaard, S. I. Bozhevolnyi, L. Markey, A. Dereux, A. V. Krasavin, P. Bolger, and A. V. Zayats, Phys. Rev. B **78**, 165431 (2008).
11. A. Boltasseva and S. I. Bozhevolnyi, IEEE J. Sel. Top. Quantum Electron. **12**, 1233 (2006).